Heliyon

Histological and biochemical evaluation of transforming growth factor-β activation and its clinical significance in patients with chronic liver disease

Hiroshi Yokoyama [a,c], Takahiro Masaki [a,*], Ikuyo Inoue [b], Mariko Nakamura [a], Yoshihiro Mezaki [a], Chisato Saeki [c], Tsunekazu Oikawa [c], Masayuki Saruta [c], Hiroyuki Takahashi [d], Masahiro Ikegami [d], Hiroshi Hano [d], Kenichi Ikejima [e], Soichi Kojima [b], Tomokazu Matsuura [a]

[a] *Department of Laboratory Medicine, The Jikei University School of Medicine, Tokyo, Japan*

[b] *Liver Cancer Prevention Research Unit, RIKEN Center for Integrative Medical Sciences, Saitama, Japan*

[c] *Division of Gastroenterology and Hepatology, Department of Internal Medicine, The Jikei University School of Medicine, Tokyo, Japan*

[d] *Department of Pathology, The Jikei University School of Medicine, Tokyo, Japan*

[e] *Department of Gastroenterology, Juntendo University Graduate School of Medicine, Tokyo, Japan*

* Corresponding author.
E-mail address: tmasaki@jikei.ac.jp (T. Masaki).

Abstract

Transforming growth factor-β (TGF-β) is a key driver for liver fibrogenesis. TGF-β must be activated in order to function. Plasma kallikrein (PLK) is a TGF-β activator that cleaves the latency-associated protein (LAP) between arginine^{58} and lysine^{59} residues and releases active TGF-β from the latent TGF-β-LAP complex. Thus, the generation of two LAP degradation products, ending at arginine^{58} (R^{58}/LAP-DPs) and beginning from lysine^{59} (L^{59}/LAP-DPs), reflects PLK-dependent TGF-β activation. However, the significance and details of TGF-β activation in patients with chronic liver disease (CLD) remain uncertain. We herein examined

the PLK-dependent TGF-β activation in patients by detecting R[58] and L[59]/LAP-DPs. A total of 234 patients with CLD were included in this study. Liver biopsy specimens were used for immunostaining to detect R[58]/LAP-DPs, while plasma samples were subjected to an enzyme-linked immunosorbent assay to measure the L[59]/LAP-DP concentration. R[58]/LAP-DP was robustly expressed in and around the sinusoidal cells before the development of the fibrous regions. The R[58]/LAP-DP expression at fibrosis stage 1 was higher than at any other stages, and the relationship between the plasma L[59]/LAP-DP level and the stage of fibrosis also showed a similar trend. The abundance of plasma L[59]/LAP-DP showed no correlation with the levels of direct serum biomarkers of liver fibrosis; however, its changes during interferon-based therapy for chronic hepatitis C were significantly associated with virological responses. Our results suggest that PLK-dependent TGF-β activation occurs in the early stages of fibrosis and that its unique surrogate markers, R[58] and L[59]/LAP-DPs, are useful for monitoring the clinical course of CLD.

Keywords: Internal medicine, Pathology

1. Introduction

Liver fibrosis is a wound-healing process characterized by the excessive accumulation of extracellular matrixes (ECMs) that results from a disturbed balance between fibrogenesis and fibrolysis [1, 2]. Because early fibrosis is often asymptomatic and can be reversed with appropriate treatment, the accurate assessment of fibrogenic activity is important for tracking and predicting disease progression and monitoring responses to antifibrotic therapies [3, 4]. Several serum biomarkers and ultrasound-based elastography are currently available for the noninvasive assessment of liver fibrosis [5, 6]. A liver biopsy is invasive but remains the gold standard for evaluating fibrosis, which is generally diagnosed based on an increased ECM deposition [6]. However, most methods basically reflect the already-accumulated ECM, and not ongoing ECM synthesis. Therefore, the development of a reliable method of assessing liver fibrogenesis, the initial event of fibrosis, is urgently needed for the management of patients with chronic liver disease (CLD).

Transforming growth factor-β (TGF-β) is a central regulator of liver fibrogenesis [4, 7]. TGF-β is secreted from liver cells in a latent form in which it is complexed with latency-associated protein (LAP) and latent TGF-β binding protein (LTBP) (Fig. 1) [8]. Several factors, including integrins, thrombospondin-1 (TSP-1), and proteases, modulate the conformation of LAPs and release active TGF-β from the latent complex in a process called TGF-β activation (Fig. 1) [8]. The resultant active TGF-β induces the transdifferentiation of quiescent hepatic stellate cells (HSCs) into myofibroblast-like activated HSCs (aHSCs), in which TGF-β-dependent Smad-
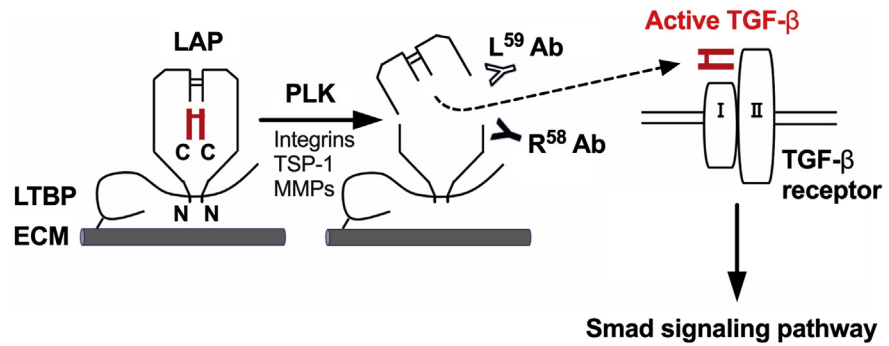
Fig. 1. PLK-dependent latent TGF-β activation and TGF-β/Smad signaling pathways. TGF-β is synthesized as a precursor protein, consisting of an N-terminal region called LAP and a C-terminal region that becomes the active TGF-β molecule, and each region dimerizes through disulfide bridges. This latent TGF-β complex is secreted from liver cells and tethered to the ECM via the LTBP. Several factors, including integrins, TSP-1, and proteases, such as PLK and matrix metalloproteinases (MMPs), act as activators of latent TGF-β in a specific manner. PLK cleaves LAP between R^{58} and L^{59}, followed by the release of active TGF-β and the generation of two LAP-DPs, each of which is recognized by R^{58} or L^{59} antibodies (Abs), respectively. Active TGF-β activates the TGF-β/Smad signaling pathway, leading to the induction of liver fibrogenesis. N and C represent the N- and C-terminus of the precursor protein, respectively.

signaling pathways are activated to stimulate ECM synthesis [1, 2, 3, 4, 7]. Although the abundance of active TGF-β in plasma and tissues appears to be an ideal biomarker that directly reflects liver fibrogenesis, its half-life in plasma is reported to be only 2−3 minutes, which makes it difficult to accurately measure the level of TGF-β [9].

Recently, Hara *et al.* have demonstrated that plasma kallikrein (PLK) cleaves LAP between the arginine[58] and lysine[59] residues to cause TGF-β activation [10]. They further showed that this event occurs in the progression of liver fibrosis in rodent models as well as in patients, by detecting the N-terminal side LAP degradation product ending at arginine[58] (R^{58}/LAP-DP) in the fibrotic liver using a specific antibody that they generated [10]. Since R^{58}/LAP-DP is covalently bound to the LTBP that is anchored to ECMs [8], the degradation products remain in tissues even after the release of active TGF-β, thereby making it possible to map TGF-β activation in the liver. The other by-product, the C-terminal side LAP-DP beginning from lysine[59] (L^{59}/LAP-DP), is released into the blood circulation after TGF-β activation, and its plasma levels can be measured with an enzyme-linked immunosorbent assay (ELISA) [11]. In animal models of liver fibrosis, the plasma L^{59}/LAP-DP abundance was well correlated with the expression of α-smooth muscle actin (α-SMA), an aHSC marker, in the liver tissue prior to the excessive deposition of ECMs [11]. In addition, L^{59}/LAP-DPs are stable in the blood, with a half-life of approximately 8 hours [11]. These data support the potential utility of R^{58} and L^{59}/LAP-DPs as surrogate markers for PLK-dependent TGF-β activation in the liver. However, there

have been very few studies focusing on the significance of TGF-β activation in the pathogenesis of liver fibrosis in patients.

In the present study, we evaluated the PLK-mediated TGF-β activation in patients with CLD by measuring the abundance of R[58] and L[59]/LAP-DPs in the liver tissues and plasma, respectively. We further examined the usefulness of the LAP-DPs as biomarkers to detect liver fibrogenesis and to monitor the clinical course of CLD.

2. Materials and methods

2.1. Patients

This study included a total of 234 patients, who had received treatment or follow-up care for CLD at Jikei University Hospital between 2007 and 2015.

For the evaluation of the R[58]/LAP-DP expression in the liver tissue, liver biopsy specimens were obtained from 89 CLD patients, consisting of 46 patients with non-alcoholic fatty liver disease (NAFLD) and 43 with viral hepatitis, of whom 19 patients were infected with hepatitis B virus (HBV) and 24 were infected with hepatitis C virus (HCV). Normal liver specimens were obtained from two living donors by needle biopsy before living-donor liver transplantation. Anthropometric measurements and laboratory tests assessing the liver function, glucose and lipid metabolism, and liver fibrosis were basically performed prior to the liver biopsy in all cases (Table 1).

For the measurement of the plasma L[59]/LAP-DP concentration, plasma specimens were collected from 188 patients, consisting of 55 patients with chronic hepatitis B (CHB), 111 patients with chronic hepatitis C (CHC), and 22 patients who had other liver diseases, such as NAFLD, autoimmune hepatitis (AIH), primary biliary cholangitis (PBC), and alcoholic liver disease, all of which were diagnosed by liver biopsy. Among the patients with viral hepatitis, 49 patients underwent a liver biopsy to assess the relationship between the plasma L[59]/LAP-DP level and histological features.

Informed consent was obtained from all patients in accordance with the Declaration of Helsinki. This study protocol was approved by the Ethics Committee of the Jikei University School of Medicine for Biomedical Research (Registration Number: 18-187 [4849], 23-134 [6595], and 25-109 [7244]).

2.2. Liver histology

Liver biopsy specimens were fixed in 10% neutral buffered formalin and paraffin-embedded. Serial 3-μm-thick sections were cut from formalin-fixed paraffin-

Table 1. Clinical and biochemical characteristics of patients who underwent a liver biopsy to evaluate the expression of R[58]/LAP-DP.

Factors	NAFLD (n = 46)	Viral hepatitis (n = 43)	*P*-value[a]
Gender (male/female)	27/19	21/22	0.35
Age (years)	48.2 ± 13.1	47.6 ± 14.1	0.78
BMI (kg/m^2)	28.6 ± 4.8	21.4 ± 2.8	<0.01
AST (U/L)	73.3 ± 45.9	74.9 ± 84.2	0.05
ALT (U/L)	116.9 ± 78.0	118.4 ± 154.6	0.05
GGT (U/L)	135.7 ± 285.6	53.5 ± 49.7	<0.01
TC (mg/dL)	208.7 ± 42.9	171.4 ± 32.1	<0.01
TG (mg/dL)	185.5 ± 109.7	109.4 ± 57.2	<0.01
HbA1c (%)	6.73 ± 1.47	5.50 ± 1.01	<0.01
ALB (g/dL)	4.34 ± 0.46	3.87 ± 0.40	<0.01
HA (ng/mL)	51.1 ± 56.8	122.8 ± 169.6	0.08
Col IV (ng/mL)	156.7 ± 53.9	166.9 ± 104.9	0.36
PLT ($\times 10^9$/L)	228.2 ± 82.2	173.9 ± 58.6	<0.01

NAFLD, non-alcoholic fatty liver disease; BMI, body mass index; AST, aspartate aminotransferase; ALT, alanine aminotransferase; GGT, γ-glutamyltransferase; TC, total cholesterol; TG, triglyceride; HbA1c, hemoglobin A1c; ALB, albumin; HA, hyaluronic acid; Col IV, type IV collagen; PLT, platelet. Data are presented as the mean $\pm$ SD.

[a] The difference in each factor between the two patient groups (NAFLD versus chronic viral hepatitis) was statistically analyzed with the Mann-Whitney U test or a chi-squared test.

embedded (FFPE) tissue specimens and subjected to hematoxylin-eosin and Masson's trichrome staining for use in histological observation.

Masson's trichrome staining stains collagen, including type I collagen (Col I), which is overproduced and a major component of the ECM in fibrotic liver (Fig. 2).

Histological grading and staging of NAFLD or chronic viral hepatitis were performed for each biopsy specimen according to the non-alcoholic steatohepatitis (NASH) Clinical Research Network criteria or the METAVIR scoring system, respectively (see Table 2 for details) [12, 13, 14].

2.3. Antibodies

Mouse monoclonal antibodies against R[58]/LAP-DP (R[58] antibody) and L[59]/LAP-DP (L[59] antibody) were generated in S. Kojima's laboratory [10]. Mouse monoclonal antibodies to detect α-SMA and cellular retinol-binding protein-1 (CRBP-1) were purchased from Dako (Glostrup, Denmark) and Santa Cruz Biotechnology (Dallas, TX), respectively. A rabbit polyclonal antibody specific for Col I was purchased from Abcam (Cambridge, UK).
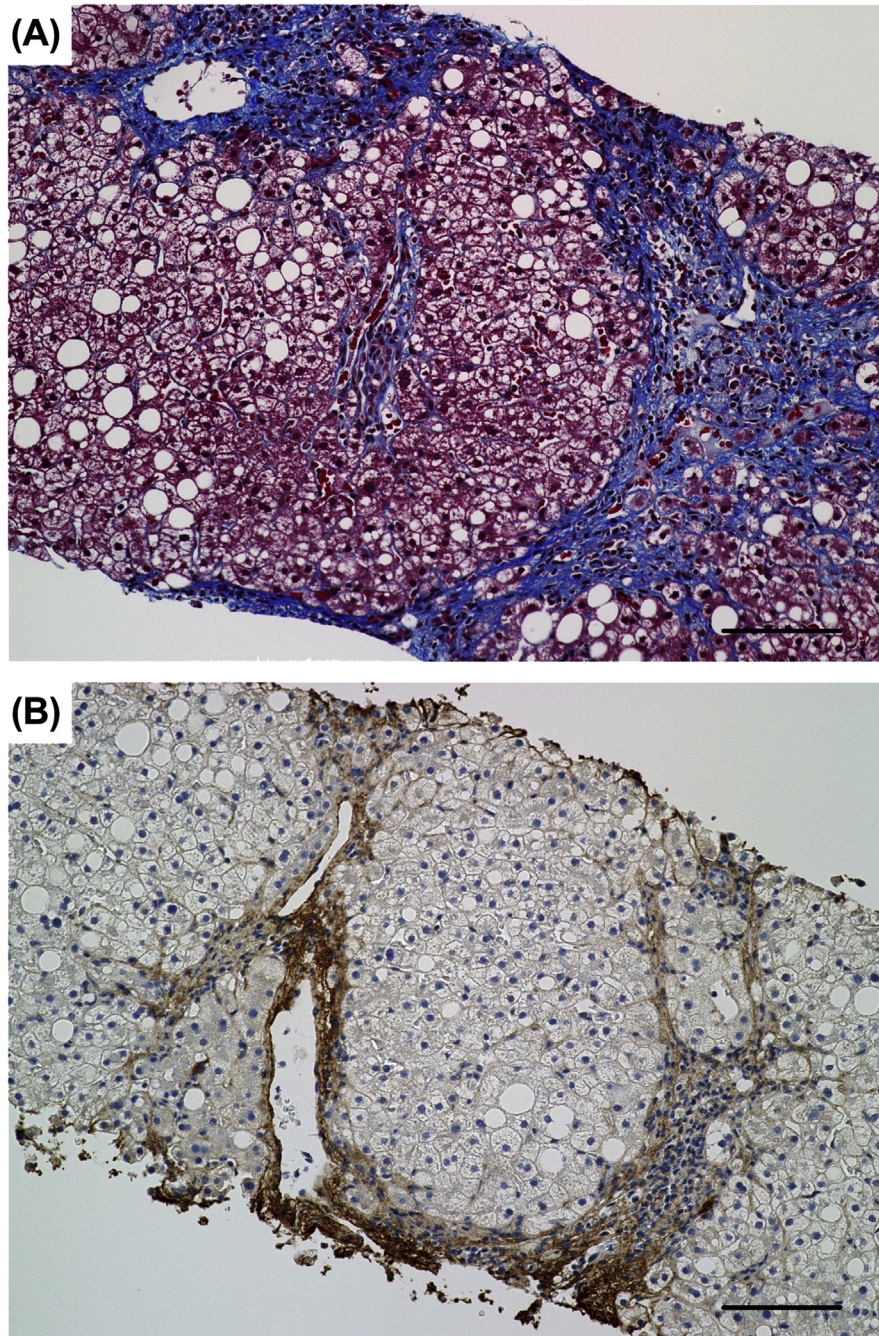
Fig. 2. The evaluation of liver fibrosis by Masson's trichrome staining and immunostaining for Col I. Serial sections of the liver biopsy specimen from a NASH patient with stage 3 fibrosis were subjected to Masson's trichrome staining (A) and immunostaining with an antibody specific for Col I (B). (A) Collagen is stained blue with Masson's trichrome staining. Collagen-containing fibrous areas are markedly observed around hepatic lobules and in periportal and perisinusoidal regions. (B) The distribution of Col I is quite similar to that of collagen shown in (A), suggesting that Masson's trichrome staining is a highly sensitive method of detecting Col I in fibrotic liver and is useful for determining the stage of liver fibrosis in CLD. Scale bars = 100 μm.

Table 2. Histological features of tissue specimens from patients who underwent a liver biopsy to evaluate the expression of R^{58}/LAP-DP.

NAFLD		Viral hepatitis	
Grade/Stage	(n)	Grade/Stage	(n)
Steatosis (%steatotic hepatocytes)			
0 (<5%)	0		
1 (5−33%)	19		
2 (>33−66%)	16		
3 (>66%)	11		
Inflammation (foci/200x field)		**Inflammation**	
0 (no foci)	2	A0 (no activity)	3
1 (<2 foci)	21	A1 (mild activity)	25
2 (2−4 foci)	17	A2 (moderate activity)	13
3 (>4 foci)	6	A3 (severe activity)	2
Ballooning			
0 (none)	11		
1 (few ballooned cells)	17		
2 (many cells/prominent ballooning)	18		
NAS			
0−2 (simple steatosis)	4		
3−4 (borderline NASH)	17		
5−8 (definitive NASH)	25		
Fibrosis		**Fibrosis**	
0 (no fibrosis)	3	F0 (no fibrosis)	3
1a (mild perisinusoidal)	11		
1b (moderate perisinusoidal)	7	F1 (portal fibrosis w/o septa)	18
1c (portal/periportal)	0		
2 (perisinusoidal and portal/periportal)	5	F2 (portal fibrosis with few septa)	17
3 (bridging fibrosis)	20	F3 (numerous septa w/o cirrhosis)	4
4 (cirrhosis)	0	F4 (cirrhosis)	1

NAFLD, non-alcoholic fatty liver disease; NAS, NAFLD activity score; NASH, non-alcoholic steatohepatitis; w/o, without. Histological grading and staging of NAFLD and chronic viral hepatitis were performed according to the NASH Clinical Research Network criteria and the METAVIR scoring system [12, 13, 14].

2.4. Immunohistochemistry

Serial 3-μm-thick sections were cut from FFPE tissue specimens for immunohistochemical staining. After deparaffinization, the sections were microwave-treated for 10 min at 95 °C for antigen retrieval and then incubated with 0.3% hydrogen peroxide in methanol for 30 min to block endogenous peroxidase activity. The sections were treated with R^{58} antibody (1 μg/mL) or L^{59}

antibody (10 μg/mL) for 30 min after incubation in phosphate-buffered saline with 0.1% Tween 20 containing 5% skim milk for 1 h to prevent nonspecific binding of antibodies. Serial sections were also used for immunostaining with an antibody against α-SMA (1/200 dilution), CRBP-1 (1/250 dilution), or Col I (1/50 dilution). Histofine Simple Stain MAX PO (Nichirei Bioscience, Tokyo, Japan) was used as a secondary antibody. In addition, New Fuchsin substrates (Nichirei Bioscience) were used for double staining. Immunoreactive signals were visualized and analyzed with a Biozero microscope (BZ-9000; Keyence, Osaka, Japan).

The R^{58}/LAP-DP expression was quantitatively evaluated by measuring the R^{58}/LAP-DP-positive areas in the entire region of each liver biopsy specimen and was represented as "% R^{58} (+) Area".

2.5. ELISA

The sandwich ELISA for L^{59}/LAP-DPs was performed according to the procedure described in a previous report [11]. Briefly, Nunc 96-well Maxisorp plates (Thermo Fisher Scientific, Waltham, MA) were coated with L^{59} antibody (20 μg/mL) in Tris-buffered saline overnight. After blocking, plasma samples were added and incubated overnight, followed by sandwiching with 1 μg/mL biotin-conjugated anti-LAP antibody for 3 h. After another 3 h of incubation with streptavidin-conjugated alkaline phosphatase (Jackson ImmunoResearch Laboratories, West Grove, PA), 4-nitrophenylphosphate disodium salt hexahydrate dissolved in diethanolamine buffer was added to each well, and the color development of the subsequent reaction was measured at 405 nm on a microplate reader. Recombinant human LAP (TGF-β1) protein (R&D Systems, Minneapolis, MN) digested with human PLK (Merck Millipore, Burlington, MA) was used for creating a standard curve.

2.6. Interferon (IFN)-based treatment for CHC

Nineteen CHC patients received a combined pegylated IFN-α (PEG-IFN-α) and ribavirin (RBV) therapy basically for 12 months. The patients were categorized into two groups in accordance with their virological responses as follows: sustained responders (SRs), continuously undetectable HCV RNA for 6 months or longer after the end of treatment, and non-responders (NRs) with detectable HCV RNA during or after treatment.

2.7. Statistical analyses

Quantitative data are shown as the mean $\pm$ standard deviation (SD). The Mann-Whitney U test or Kruskal-Wallis test was employed to evaluate differences in the abundance of LAP-DPs between two groups or more than two groups,

respectively. A chi-squared test was used to compare the distribution of categorical variables between two groups. Pearson's correlation coefficient was determined to examine the degree of correlation between two variables. The Wilcoxon matched-pairs signed rank test was used to analyze the changes in the plasma L[59]/LAP-DP level during treatment. *P*-values of <0.05 were considered to be statistically significant.

3. Results

3.1. Characteristics of patients who underwent a liver biopsy for the evaluation of the R[58]/LAP-DP expression

The clinical and biochemical characteristics of 89 patients (46 patients with NAFLD and 43 with chronic viral hepatitis), who underwent a liver biopsy to evaluate the expression of R[58]/LAP-DP, are shown in Table 1. There were no statistically significant differences regarding age, gender, or the serum levels of liver enzymes, aspartate aminotransferase (AST) and alanine aminotransferase (ALT), between the patients with NAFLD and those with viral hepatitis. The body mass index (BMI), serum concentrations of γ-glutamyltransferase (GGT), total cholesterol (TC), and triglyceride (TG), and the blood hemoglobin A1c (HbA1c) level in the NAFLD patients were significantly higher than those in the viral hepatitis patients, showing that the development of NAFLD is strongly associated with disturbances in lipid and glucose metabolism. Significant reductions in serum albumin (ALB) and the number of platelets (PLTs), as well as the elevation of serum fibrosis markers, hyaluronic acid (HA), and type IV collagen (Col IV), were observed in patients with viral hepatitis. However, the serum levels of these fibrosis markers in the two patient groups did not differ to a statistically significant extent.

The histological findings of liver biopsy specimens from the patients are presented in Table 2. In contrast to the differences in the laboratory characteristics (Table 1), there appeared to be no obvious differences in the distribution of the grades of inflammation or the stages of fibrosis between the two patient groups.

3.2. The expression and distribution of R[58]/LAP-DP in the liver tissue of patients with NAFLD

Liver biopsy specimens from patients with NAFLD were subjected to Masson's trichrome staining, which stains Col I (Fig. 2), and immunostaining with an antibody specific for R[58]/LAP-DP or α-SMA, a marker of aHSCs and myofibroblasts (Fig. 3). In liver specimens from living donors (negative controls; NC) and patients with stage 0 fibrosis, no parenchymal regions were specifically stained with Masson's trichrome or α-SMA antibody, with the exception of the portal areas
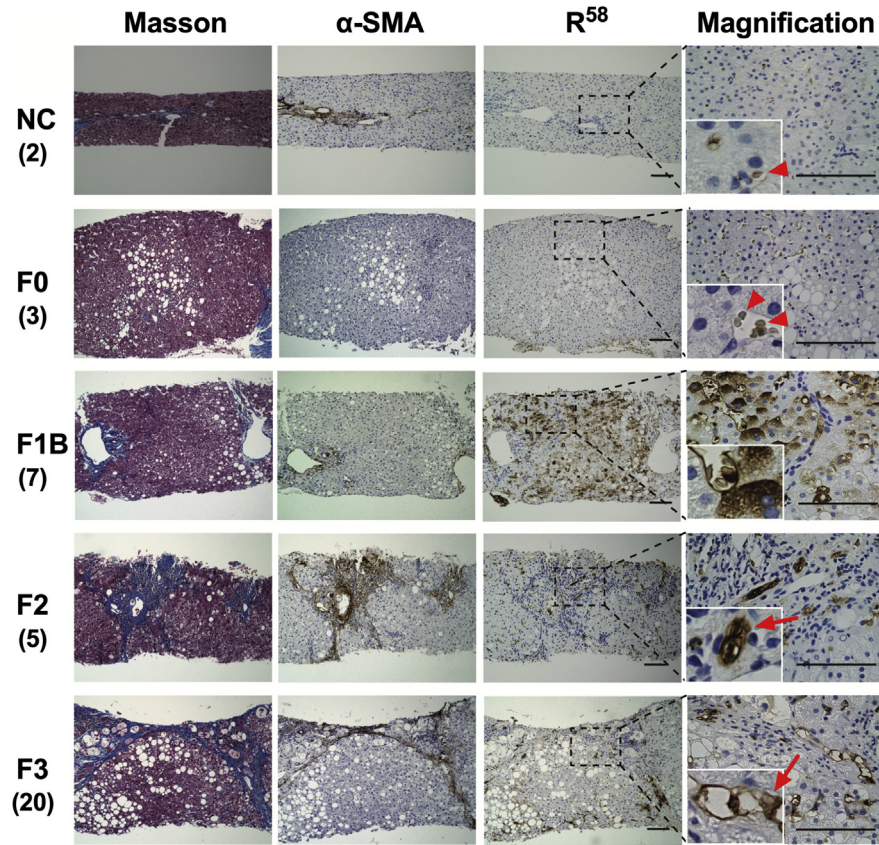
Fig. 3. Immunohistochemical staining of liver biopsy specimens from patients with NAFLD. Liver biopsy specimens from living donors (NC) and NAFLD patients with the indicated stages of fibrosis (F0-3) were stained with Masson's trichrome and an antibody against α-SMA or R^{58}/LAP-DP (R^{58}). The magnification images are derived from the black dashed squares. Insets show enlarged images of the representative areas. Arrowheads show non-specific staining of red blood cells by an R^{58} antibody. Arrows indicate R^{58}/LAP-DP-positive sinusoidal cells and adjacent fibrous matrices. Tissue sections shown are representative of multiple biopsy samples, and the numbers in parentheses indicate the number of samples for each fibrosis stage. Scale bars = 100 μm.

containing vessels and connective tissues (Fig. 3, top panels and second panels from the top). Mild steatosis was only present in liver tissue from patients with stage 0 fibrosis; however, no apparent expression of R^{58}/LAP-DP was observed in the liver parenchyma. Negligible non-specific staining of red blood cells by R^{58} antibody was detected under high-magnification (arrowheads). In biopsy specimens from patients with stage 1B fibrosis, mild steatosis and fibrosis were observed in centrizonal regions, while R^{58}/LAP-DP was robustly expressed throughout hepatic lobules (Fig. 3, third panels from the top). The R^{58}/LAP-DP expression was mostly detected along the sinusoidal walls and on adjacent hepatocytes by observation under higher magnification. Obvious periportal and bridging fibrosis was present in liver specimens from fibrosis stage 2 and 3 patients, respectively (Fig. 3, fourth and fifth panels from the top). The R^{58}/LAP-DP expression

was globally reduced and primarily distributed in and around the regions of fibrosis. Under high magnification, R^{58}/LAP-DP signals were mainly detected along sinusoidal walls and on the adjacent fibrous matrices (arrows).

To more precisely assess the expression and localization of R^{58}/LAP-DP in the liver tissue, we performed double-immunostaining of the liver biopsy specimens obtained from NAFLD patients with stage 1B and 3 fibrosis (Fig. 4). The sections were coimmunostained with antibodies against R^{58}/LAP-DP and CRBP-1, which is a marker specific for both aHSCs and quiescent HSCs [15, 16]. Similar to the results shown in Fig. 3, R^{58}/LAP-DP was markedly expressed along the sinusoidal walls containing CRBP-1-positive HSCs (Fig. 4B and D, arrows). The R^{58}/LAP-DP expression was also detected on some hepatocytes in the liver tissue from a fibrosis stage 1B patient (Fig. 4B, arrowheads).

Collectively, our histological observation of NAFLD liver tissues showed that R^{58}/LAP-DP was robustly expressed on and around sinusoidal cells before the completion of liver fibrosis, suggesting that the expression of R^{58}/LAP-DP may reflect fibrogenic activity in the early stages of NAFLD.
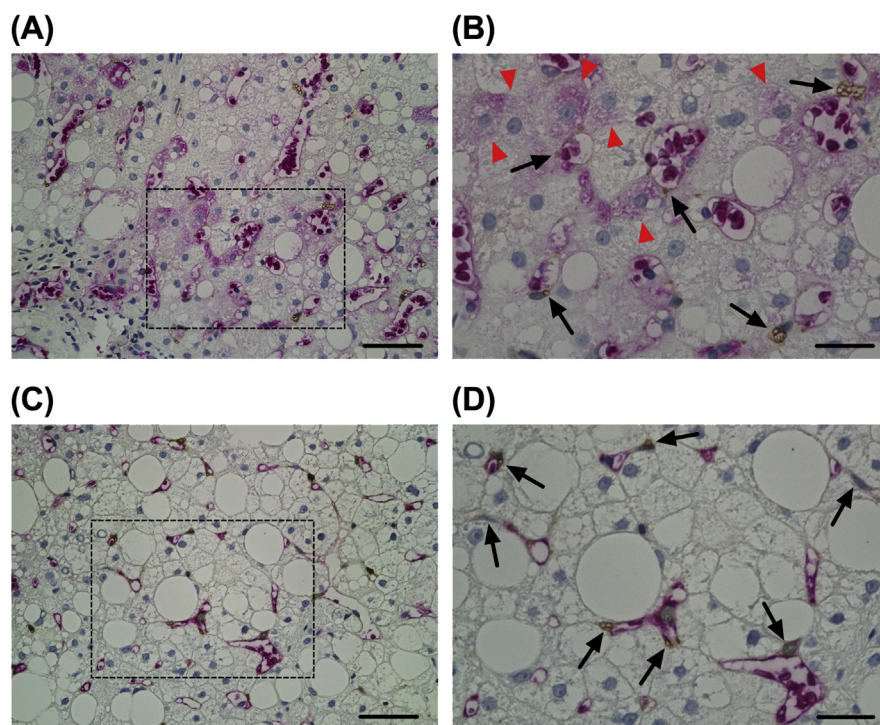

Fig. 4. The expression and localization of R^{58}/LAP-DP in the liver tissues of NAFLD patients. Liver biopsy specimens from NAFLD patients with F1B (A and B) and F3 (C and D) were coimmunostained with antibodies against R^{58}/LAP-DP (red) and CRBP-1 (brown). Panels (B) and (D) are enlarged images of the black dashed squares in panels (A) and (C), respectively. Arrowheads indicate hepatocytes positive for R^{58}/LAP-DP, while arrows indicate HSCs. Scale bars in panels (A) and (C) = 50 μm. Scale bars in panels (B) and (D) = 20 μm.

3.3. The expression and distribution of R^{58}/LAP-DP in the liver tissue of patients with chronic viral hepatitis

We next examined the liver biopsy specimens from patients with chronic viral hepatitis using the same method as for NAFLD (Fig. 5). In specimens from patients with a METAVIR score of F0, R^{58}/LAP-DP was marginally expressed within the hepatic lobules and was found to be mainly localized along the sinusoidal walls by
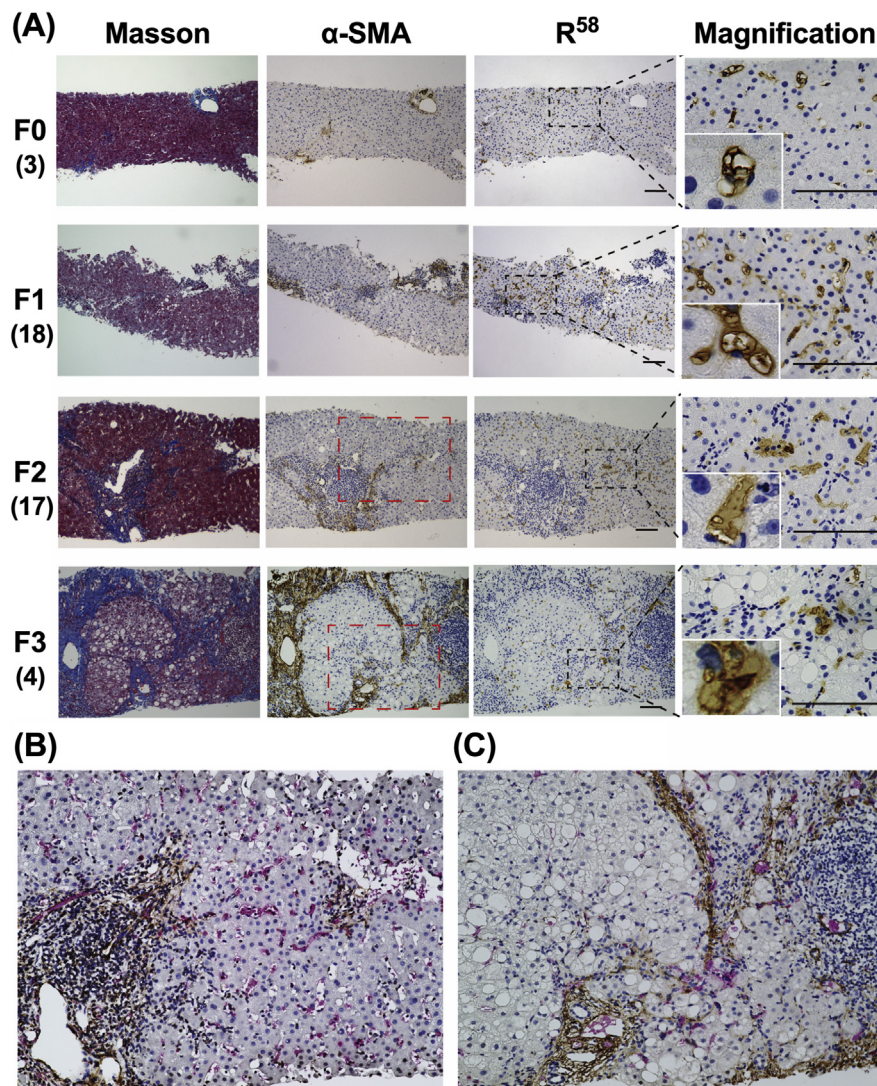

Fig. 5. Immunohistochemical staining of liver biopsy specimens from patients with viral hepatitis. (A) Liver biopsy specimens from patients with viral hepatitis (F0-3) were stained with Masson's trichrome and an antibody against R^{58}/LAP-DP (R^{58}) or α-SMA. The magnification images are derived from the black dashed squares. Insets show enlarged images of the representative areas. Tissue sections shown are representative of multiple biopsy samples, and the numbers in parentheses indicate the number of samples for each fibrosis stage. Scale bars = 100 μm. (B and C) Liver biopsy specimens from F2 and F3 patients were coimmunostained with antibodies against R^{58}/LAP-DP (red) and α-SMA (brown). Panels (B) and (C) are enlarged images of red dashed squares in F2 and F3 panels, respectively.

observation under high magnification (Fig. 5A, top panels). In biopsy specimens from F1 stage patients, mild periportal fibrosis was observed with Masson's trichrome and α-SMA staining (Fig. 5A, second panels from the top). R^{58}/LAP-DP was detected extensively throughout the liver parenchyma, but its expression was weaker and more scattered than that in NAFLD livers with a comparable stage of fibrosis. R^{58}/LAP-DP signals were largely observed along the sinusoidal walls but were rarely detected on hepatocytes by high-magnification imaging. Interestingly, the distribution of R^{58}/LAP-DP was quite different from that of α-SMA in this stage. Apparent periportal and septal fibrosis with moderate necroinflammation was observed in biopsy specimens from F2 and F3 stage patients (Fig. 5A, third and fourth panels from the top). Similar to NAFLD livers, the overall R^{58}/LAP-DP expression was attenuated in comparison to that in F1 tissues and was predominantly detected in and around the regions of fibrosis. The R^{58}/LAP-DP signals appeared to be less associated with necroinflammation. High-magnification images of F2 and F3 specimens showed that R^{58}/LAP-DP was mainly expressed in sinusoidal cells and adjacent fibrous matrices. Double-staining experiments further demonstrated that R^{58}/LAP-DP-positive sinusoidal cells were present around and between the α-SMA-positive fibrous regions, as though the cells mediated the formation of septal fibrosis (Fig. 5B and C). These results suggest that R^{58}/LAP-DP might be a histological marker for evaluating the fibrogenic potential in the early stages of liver fibrosis.

3.4. The relationship between PLK-dependent TGF-β activation and the histological features of the liver tissue of NAFLD and chronic viral hepatitis patients

Our histological observations showed that PLK-mediated TGF-β activation was obviously detected in the early stages of liver fibrosis, while TGF-β signaling has been reported to be associated not only with fibrosis but also with the lipid accumulation or inflammatory cell infiltration [17]. To more accurately validate the significance of PLK-dependent TGF-β activation in the progression of CLDs, we examined the relationship between the R^{58}/LAP-DP expression and the histological findings in all biopsy samples. A quantitative evaluation of the R^{58}/LAP-DP expression was performed as shown in the Materials and methods. Distinct R^{58}/LAP-DP deposition was frequently observed at the edge of biopsy tissues, regardless of the histological findings, presumably resulting from tissue crushing by a needle biopsy or non-specific staining by R^{58} antibody (Fig. 6A, left panel, arrows). To eliminate this effect, areas less than 100 μm from the edge were excluded from measurement (Fig. 6A, right panel).

The percentages of R^{58}/LAP-DP-positive areas in all biopsy specimens from patients with NAFLD or viral hepatitis ranged from 1.00% to 27.1% (average, 6.20%). In contrast, the percentages in the biopsy specimens from the two living donors were
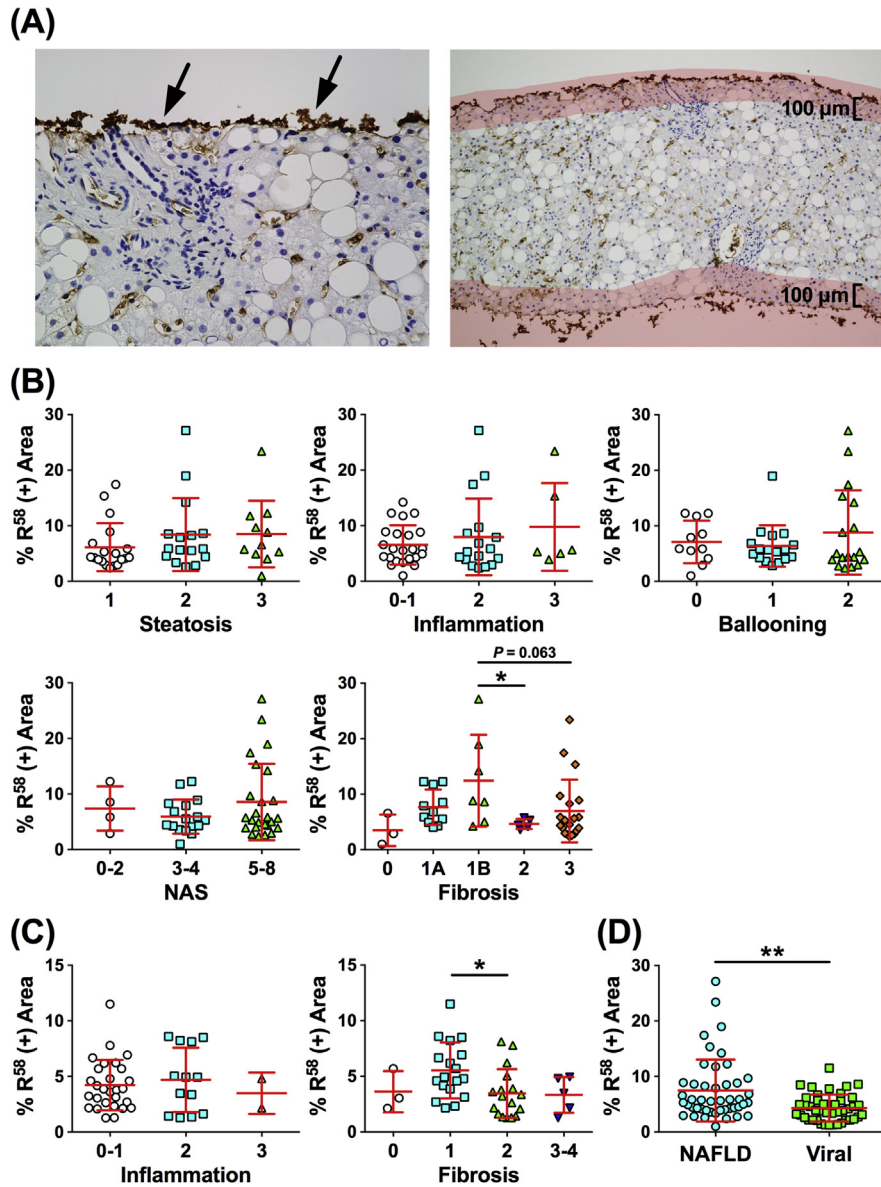
Fig. 6. Correlation between the R^{58}/LAP-DP expression and histological findings of the liver in patients with NAFLD or viral hepatitis. (A) R^{58}/LAP-DP deposition is observed at the edge of the biopsy specimens (arrows, left panel), resulting from tissue crushing during a needle biopsy or non-specific staining by R^{58} antibody. To eliminate this effect, the area less than 100 μm from the edge (shaded with pale red) was excluded from measurement (right panel). (B) The relationship between the R^{58}/LAP-DP expression and the scores for steatosis, lobular inflammation, hepatocellular ballooning, NAS, or fibrosis in patients with NAFLD. (C) The relationship between the R^{58}/LAP-DP expression and the degree of inflammation or fibrosis in patients with viral hepatitis. (D) A comparison of the R^{58}/LAP-DP expression between patients with NAFLD and those with viral hepatitis. The extent of the R^{58}/LAP-DP expression is represented as "% R^{58} (+) Area" in panels (B–D). The results shown represent the mean ± SD. Each dot represents the value for one patient. The Mann-Whitney U test and Kruskal-Wallis test were used for the statistical analyses. *$P < 0.05$, **$P < 0.01$.

1.29% and 1.88%, respectively (average, 1.58%). In NAFLD liver tissues, the extent of the R^{58}/LAP-DP expression did not show a statistically significant association with the scores for steatosis, lobular inflammation, hepatocellular ballooning, or the NAFLD activity score (NAS) (Fig. 6B). Regarding the relationship with the fibrosis stages, the R^{58}/LAP-DP expression was the highest at the 1B stage; more than 10% of the entire section was R^{58}/LAP-DP-positive (Fig. 6B, "Fibrosis" panel). The expression clearly decreased at stages 2 and 3, and especially, a statistically significant difference was observed between stages 1B and 2 ($P < 0.05$). In the liver tissue specimens with viral infection, there were no marked differences in the R^{58}/LAP-DP expression among the grades of inflammation (Fig. 6C, left panel). Similar to the results obtained from NAFLD liver tissue, the R^{58}/LAP-DP expression at the F1 stage was higher than that at any other stages of fibrosis, and the expression decreased at the F2 and F3 stages. A statistically significant difference was found between the F1 and F2 stages (Fig. 6C, right panel; $P < 0.05$). Interestingly, the percentages of R^{58}/LAP-DP-positive areas were substantially higher in the liver tissues of NAFLD patients than in those of patients with viral infection (7.49 ± 5.58% versus 4.08 ± 2.50%, mean ± SD; $P < 0.01$) (Fig. 6D), although there was no marked difference in the distribution of fibrosis stages between the two patient groups (Table 2).

These statistical analyses provide evidence that PLK-dependent TGF-β activation is associated with liver fibrosis and it occurs in the early stages, regardless of the causes of CLD. However, there appears to be a difference in the extent of TGF-β activation among different etiologies of CLD.

3.5. The characteristics of patients who underwent blood testing for the measurement of the plasma L^{59}/LAP-DP concentration

The clinical and biochemical characteristics of 188 patients with CLD, who underwent a blood test to measure their plasma L^{59}/LAP-DP concentration, are shown in Table 3. The female ratio was significantly higher among patients with other liver diseases (especially AIH and PBC) than in those with CHB or CHC. The age distributions of the three patient groups were widely different from one another. With respect to blood markers and tests closely linked to the liver function or tumorigenesis, differences in the serum levels of ALB, AST, ALT, GGT, or protein induced by vitamin K absence-II (PIVKA-II) were not pronounced, but the serum α-fetoprotein (AFP) levels, PLT counts, and the prothrombin time (PT) differed significantly among the three groups. The significant elevation of the serum levels of fibrosis markers, such as HA and Col IV, and the fibrosis index based on the four factors (FIB-4) [18] was observed in patients with CHC. There was no significant difference in the plasma L^{59}/LAP-DP concentration among the three groups.

Table 3. Clinical and biochemical characteristics of patients who underwent a blood test to measure the plasma L^{59}/LAP-DP concentration.

Factors	CHB (n = 55)	CHC (n = 111)	Others (n = 22)	*P*-value[a]
Gender (male/female)	31/24	56/55	5/17	<0.05
Age (years)	43.6 ± 12.7	59.6 ± 12.4	51.4 ± 11.0	<0.01
ALB (g/dL)	4.19 ± 0.40	4.02 ± 0.50	4.00 ± 0.43	0.09
AST (U/L)	126.8 ± 279.5	54.84 ± 42.10	49.82 ± 34.38	0.36
ALT (U/L)	263.0 ± 586.2	65.66 ± 80.42	67.05 ± 60.74	0.89
GGT (U/L)	83.35 ± 108.9	58.93 ± 49.94	115.1 ± 157.1	0.43
HA (ng/mL)	73.18 ± 110.6	268.1 ± 366.8	100.7 ± 125.6	<0.01
Col IV (ng/mL)	141.1 ± 67.80	206.1 ± 131.3	143.2 ± 57.03	<0.01
AFP (ng/mL)	10.49 ± 38.16	10.27 ± 9.898	22.00 ± 50.68	<0.01
PIVKA-II (mAU/mL)	17.88 ± 5.152	47.11 ± 212.5	19.50 ± 6.565	0.87
PLT ($\times 10^9$/L)	190.5 ± 55.72	143.0 ± 52.10	214.1 ± 49.96	<0.01
PT (%)	92.33 ± 7.756	89.45 ± 12.50	96.82 ± 5.404	<0.05
FIB-4	1.684 ± 1.095	3.903 ± 3.962	1.665 ± 0.8910	<0.01
L^{59}/LAP-DP (pM)	141.0 ± 125.4	134.4 ± 115.8	130.4 ± 114.1	0.94

CHB, chronic hepatitis B; CHC, chronic hepatitis C; ALB, albumin; AST, aspartate aminotransferase; ALT, alanine aminotransferase; GGT, γ-glutamyltransferase; HA, hyaluronic acid; Col IV, type IV collagen; AFP, α-fetoprotein; PIVKA-II, protein induced by vitamin K absence-II; PLT, platelet; PT, prothrombin time; FIB-4, fibrosis index based on the four factors; L^{59}/LAP-DP, degradation product of latency-associated protein beginning from lysine[59]. Data are presented as the mean ± SD.

[a] The difference in each factor among the three patient groups (CHB, CHC, and others) was statistically analyzed with the Kruskal-Wallis test or a chi-squared test.

3.6. The abundance of L^{59}/LAP-DPs in the liver tissue and the relationship between the plasma concentration and the liver histology of chronic viral hepatitis patients

To test whether L^{59}/LAP-DPs are detected in liver tissue following PLK-dependent TGF-β activation, serial sections of the liver biopsy specimen from a CHB patient with F2 stage were immunostained with an antibody against L^{59}/LAP-DP using the same method as with R^{58} antibody. The expression of R^{58}/LAP-DP was observed in and around portal areas and along the fibrous septa (Fig. 7A, left panel). This suggests that PLK-dependent TGF-β activation occurs in the patient liver. However, L^{59}/LAP-DP signals were rarely detectable in the liver tissue (Fig. 7A, right panel), indicating that L^{59}/LAP-DPs could be released into the blood and could be used as a blood biomarker reflecting the TGF-β activation in the liver.

Next, to examine the relationship between the plasma concentration of L^{59}/LAP-DP and the histological features of the liver tissue, 49 patients with CHB or CHC underwent a liver biopsy. The histological findings of the biopsy specimens are presented in Table 4. Although the inflammatory activities of the CHB patients' livers were significantly more severe than those of the CHC patients' livers, no
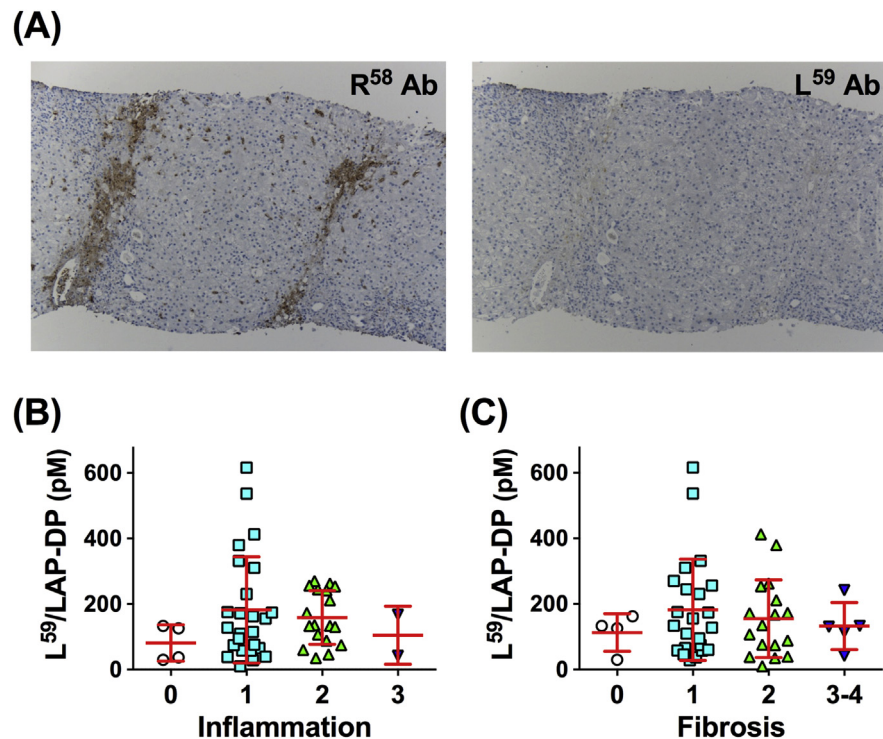
Fig. 7. The abundance of L^{59}/LAP-DPs in the liver tissue and association of the plasma level with the histological findings of liver specimens from chronic viral hepatitis patients. (A) Serial sections of the liver biopsy specimen from a CHB patient with F2 stage were immunostained with an antibody against R^{58}/LAP-DP (R^{58} Ab, left panel) or L^{59}/LAP-DP (L^{59} Ab, right panel). (B and C) The relationship between the plasma L^{59}/LAP-DP level and the degree of inflammation (B) or fibrosis (C) in patients with chronic viral hepatitis. The results shown represent the mean $\pm$ SD. Each dot represents the value for one patient. The Kruskal-Wallis test was used for the statistical analyses.

obvious difference in the distribution of the fibrosis stages was found between the two patient groups. The average plasma concentration of L^{59}/LAP-DP in patients with inflammatory grade 1 was higher than that in patients with other grades, but there was no significant difference in the distribution of the plasma abundance between any patient group with a different grade (Fig. 7B). A similar trend was observed among patients with different fibrosis stages; that is, the average plasma level of L^{59}/LAP-DP was the highest in patients with stage 1 (Fig. 7C), consistent with the results of the R^{58}/LAP-DP expression in the patients' livers (Fig. 6B and C, "Fibrosis" panels).

3.7. The relationship between the plasma L^{59}/LAP-DP level and factors associated with the liver function, fibrosis, or carcinogenesis in patients with CLD

To explore the possible use of the plasma L^{59}/LAP-DP abundance as a biomarker for liver fibrosis, its relationship with factors related to the liver function was examined

Table 4. The histological features of the liver biopsy specimens from patients who underwent a blood test to measure the plasma L^{59}/LAP-DP concentration.

Grade/Stage	CHB (n)	CHC (n)	P-value[a]
Inflammation			
A0 (no activity)	1	3	
A1 (mild activity)	6	19	<0.05
A2 (moderate activity)	10	8	
A3 (severe activity)	2	0	
Fibrosis			
F0 (no fibrosis)	1	3	
F1 (portal fibrosis w/o septa)	7	16	
F2 (portal fibrosis with few septa)	9	8	0.63
F3 (numerous septa w/o cirrhosis)	1	2	
F4 (cirrhosis)	1	1	

CHB, chronic hepatitis B; CHC, chronic hepatitis C; w/o, without.

[a] The difference in the distribution of the grades of inflammation or the stages of fibrosis between the two patient groups (CHB versus CHC) was statistically analyzed with a chi-squared test.

in CLD patients. The plasma L^{59}/LAP-DP level showed no significant relationship with gender, age, PT, PLT count, or the serum concentrations of AST, ALT, or GGT, but a statistically significant negative correlation was observed between the plasma L^{59}/LAP-DP level and the abundance of serum ALB (Pearson's $r = -0.172$, $P = 0.018$) (Fig. 8A−H). We further tested whether the plasma L^{59}/LAP-DP concentration was related to serum biomarkers that are closely linked to liver fibrosis or cancer. There was no obvious association between the plasma L^{59}/LAP-DP level and the serum abundance of HA, Col IV, AFP, or PIVKA-II. However, a weak but non-negligible positive correlation was found between the plasma L^{59}/LAP-DP level and the FIB-4 value (Pearson's $r = 0.156$, $P = 0.032$) (Fig. 9A−E). These results suggest that the abundance of L^{59}/LAP-DP is associated with liver fibrosis because serum ALB and FIB-4 values are known to have a close relationship to the progression of liver fibrosis [5, 18, 19, 20]. However, the role of L^{59}/LAP-DPs in the development of liver fibrosis might be different from the roles of HA and Col IV, which are widely used as serum fibrosis markers.

3.8. The prediction of the viral response to IFN-based therapy in CHC patients based on the abundance of plasma L^{59}/LAP-DP

Several studies have shown that significant reductions in the serum levels of liver fibrosis markers are observed in SRs among patients who have received treatment for CHC [21, 22, 23]. To clarify whether the plasma L^{59}/LAP-DP abundance serves as a predictive marker for viral responses to antiviral treatment, its association with treatment outcomes was examined in CHC patients who received combined PEG-IFN-α and RBV treatment. As shown in Fig. 10A, the plasma L^{59}/
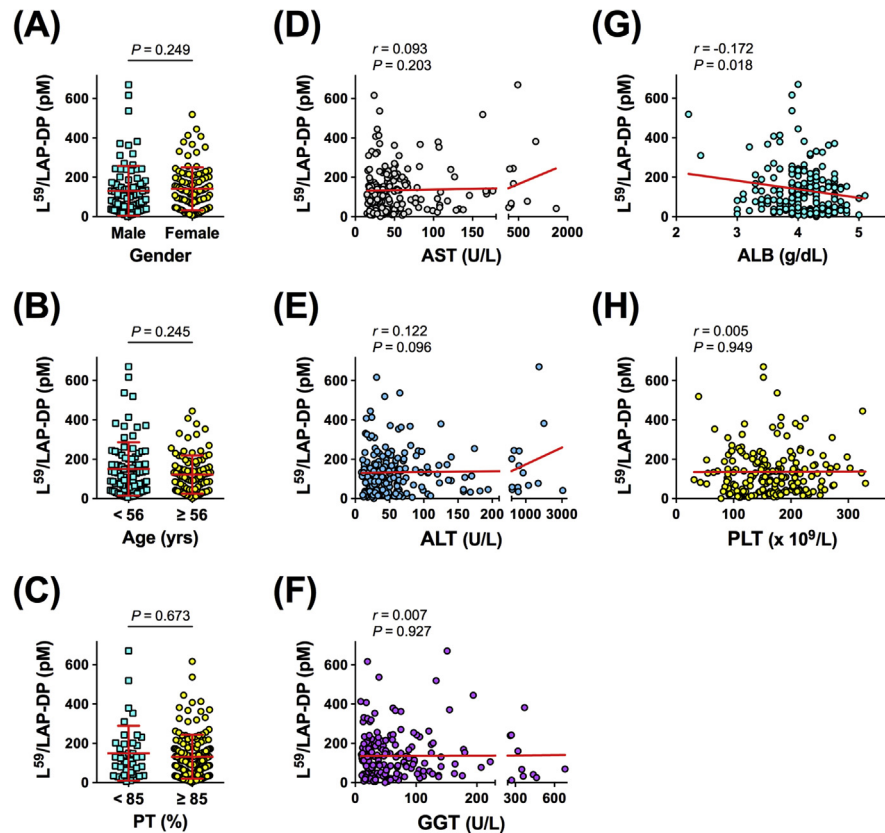
Fig. 8. Correlation between the plasma L^{59}/LAP-DP level and factors related to the liver function in patients with CLD. The plasma concentration of L^{59}/LAP-DP was measured by an ELISA, and its correlations with gender (A), age (B), and the values of blood tests or markers reflecting the liver function, such as PT (C), AST (D), ALT (E), GGT (F), ALB (G), and PLT (H), were examined. Each dot represents the value for one patient. The Mann-Whitney U test and Pearson's correlation coefficient (r) were used for the statistical analyses of panels (A−C) and panels (D−H), respectively.

LAP-DP level at 6 months after the beginning of treatment was lower in comparison to before treatment (82.67 ± 54.17 pM versus 114.9 ± 81.06 pM, mean ± SD), but the difference was not statistically significant ($P = 0.11$). The plasma concentrations of L^{59}/LAP-DP in SRs and NRs prior to treatment were 129.1 ± 72.25 pM and 84.07 ± 97.26 pM (mean ± SD), respectively, and those after 6 months of treatment were 76.60 ± 47.78 pM and 95.84 ± 69.13 pM (mean ± SD), respectively. There were no significant differences in the plasma L^{59}/LAP-DP levels before or after the initiation of treatment between SRs and NRs. Concerning the relationship between changes in the plasma L^{59}/LAP-DP concentration during IFN-based treatment and the treatment outcomes, 11 of 13 SRs showed a decreased plasma L^{59}/LAP-DP abundance at 6 months after the initiation of treatment, while five of 6 NRs exhibited an increase. There was a statistically significant difference in the SR-to-NR ratio between the two patient groups categorized based on changes in the plasma L^{59}/LAP-DP level (Fig. 10B). To more precisely
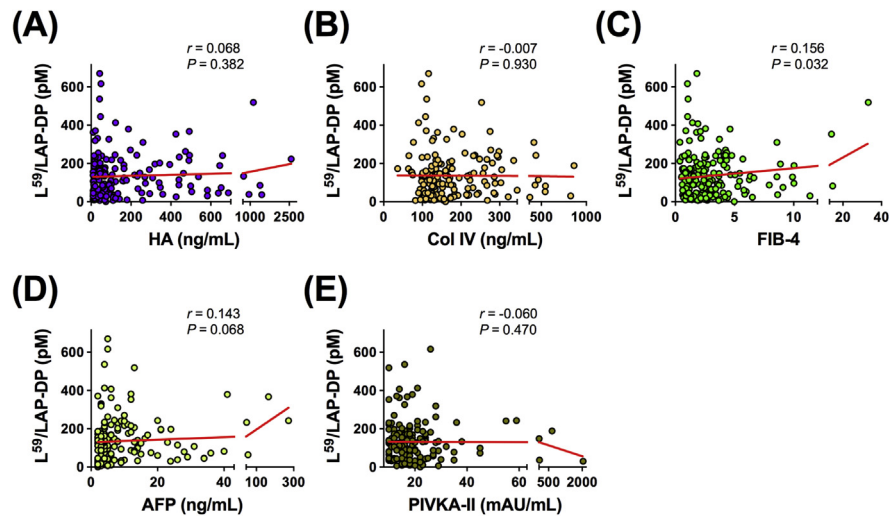
Fig. 9. Correlation between the plasma L^{59}/LAP-DP level and the serum concentrations of fibrosis and tumor markers in patients with CLD. The plasma abundance of L^{59}/LAP-DP was measured by an ELISA, and its correlations with the serum levels of fibrosis markers, HA (A), CoI IV (B), the FIB-4 value (C), and the levels of tumor markers, AFP (D) and PIVKA-II (E), were tested. Each dot represents the value for one patient. Pearson's correlation coefficient (r) was determined in the statistical analyses.

assess the predictive value of L^{59}/LAP-DPs in relation to the treatment outcome, the time-course changes in the plasma L^{59}/LAP-DP level were analyzed in individual patients. A representative case from the SR group demonstrated that the plasma L^{59}/LAP-DP abundance decreased rapidly and remained low after the initiation of combined PEG-IFN-α and RBV therapy, whereas more delayed and incomplete declines were observed in the serum levels of HA and AFP (Fig. 10C), both of which are reported to be serum markers for predicting the outcomes of treatment in patients with CHC [21, 22, 23, 24]. In a representative case from the NR in which serum HCV RNA reappeared just after the end of treatment, the plasma L^{59}/LAP-DP level fluctuated and was gradually elevated even during treatment, although the serum concentrations of HA and AFP were decreased after the beginning of treatment (Fig. 10D).

These results suggest that the plasma L^{59}/LAP-DP abundance and its changes are useful as blood biomarkers for predicting the outcomes of IFN-based treatment for CHC. Its predictive accuracy, including sensitivity and reliability, could be higher in comparison to serum HA and AFP.

4. Discussion

In the current study, we examined the abundance of R^{58} and L^{59}/LAP-DPs in patients with CLD and revealed the significance of PLK-dependent TGF-β activation
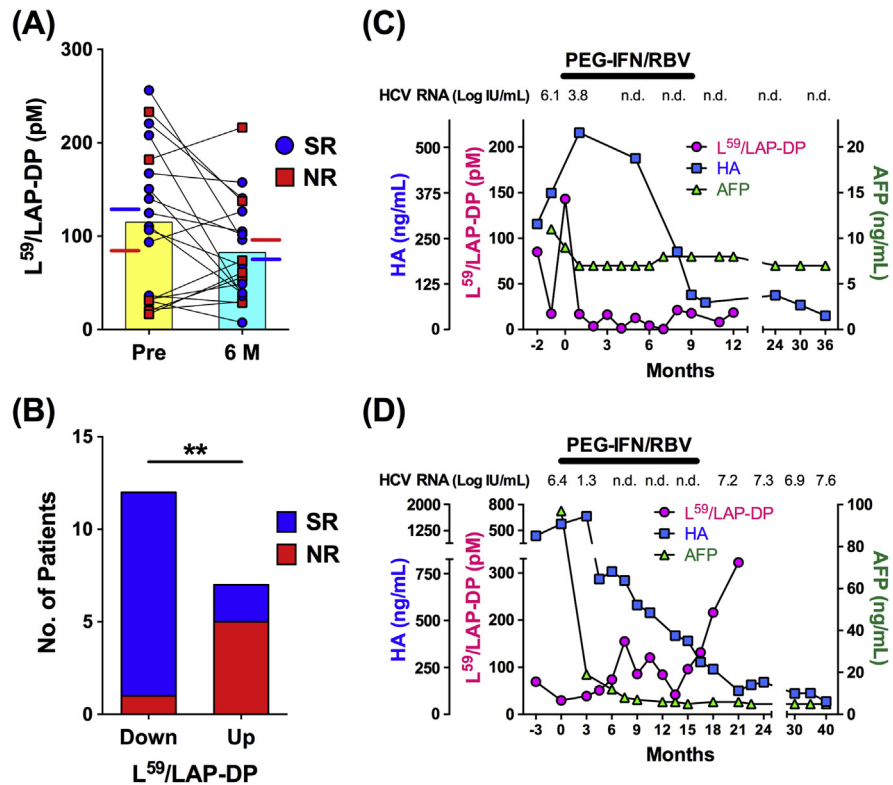
Fig. 10. Changes in the plasma L^{59}/LAP-DP level during interferon-based treatment for CHC and the relationship with the treatment outcome. (A) The plasma L^{59}/LAP-DP level before and at 6 months after the initiation of treatment was measured in 19 CHC patients who received IFN-based treatment. The significance of the changes was analyzed with the Wilcoxon matched-pairs signed rank test. Each symbol represents the value for one patient, and symbols for an identical patient are linked with a line. Patients with blue circles or red squares indicate SRs or NRs, respectively (defined in the Materials and methods). The yellow and the pale blue bars represent the mean plasma levels of L^{59}/LAP-DP in 19 patients before and at 6 months after the beginning of treatment, respectively. The blue and the red lines indicate the mean plasma concentrations of L^{59}/LAP-DP in SRs and NSs, respectively. (B) The relationship between the changes in the plasma L^{59}/LAP-DP level during IFN-based treatment and the treatment outcome was statistically analyzed with a chi-squared test. "Down" and "Up" indicate that plasma L^{59}/LAP-DP levels are lower and higher, respectively, at 6 months after the beginning of treatment in comparison to before treatment. The blue and red bars represent the numbers of SRs and NRs, respectively. **$P < 0.01$. (C and D) Changes in the plasma L^{59}/LAP-DP level and serum concentrations of HA and AFP during and after combination therapy with PEG-IFN-α and RBV (PEG-IFN/RBV) were examined. The panels (C) and (D) are representative cases from the SR and the NR, respectively. n.d., not detected.

in the early stages of liver fibrosis. The robust expression of R^{58}/LAP-DP was detected in and around sinusoidal cells before the development of α-SMA-positive fibrous regions, suggesting that PLK-dependent TGF-β activation may be the initial event that induces liver fibrogenesis. A previous study showed that R^{58}/ LAP-DP was mainly detected in α-SMA-positive areas in liver tissues from both rodent models and patients with advanced fibrosis [10]. This was consistent with

our histological findings at fibrosis stages 2 and 3, but not at earlier stages, in which the distribution of R[58]/LAP-DP was different from that of α-SMA (Figs. 3 and 5). Our closer immunohistochemical analysis further revealed that R[58]/LAP-DPs were mostly expressed in α-SMA-negative sinusoidal cells existing around and between the α-SMA-positive fibrous areas, as though the R[58]/LAP-DP expression predicted the subsequent progression of fibrosis (Fig. 5B and C). These results suggest that the R[58]/LAP-DP expression can reflect the active TGF-β production that causes liver fibrogenesis and may function as a predictive marker of the fibrogenic activity at the early stages of fibrosis. This was the case with the relationship between the plasma L[59]/LAP-DP level and the fibrosis stage in patients. The average plasma concentration of L[59]/LAP-DP was highest in patients with stage 1; however, its difference among patient groups with different fibrosis stages was not so pronounced (Fig. 7C). The contribution of PLK-mediated TGF-β activation to fibrosis in the early stages was also reported in a previous study using mouse models of liver fibrosis [11].

The latent TGF-β complex secreted from cells is typically tethered to the ECM via LTBPs [8]. PLK or other molecules, including integrins, TSP-1, and proteases, such as matrix metalloproteinases, are known to liberate active TGF-β from the LAP in a specific manner [8]. Since part of the LAP remains in the liver tissue, even after the release of active TGF-β, PLK-cleaved R[58]/LAP-DPs were expected to be mainly detected in the ECM. However, our immunostaining data demonstrated that the R[58]/LAP-DP expression was not marked in the ECM or at advanced stages of fibrosis with excessive ECM deposition (Figs. 3 and 5A, fibrosis stages 2 and 3). Weng et al. showed that activation of the TGF-β signaling pathway was positively correlated with the severity of liver fibrosis in patients with HBV infection and NAFLD [25], suggesting that factors other than PLK contribute to TGF-β activation in the advanced stages of fibrosis. Levels of activators of latent TGF-β, including integrins (e.g. integrin αvβ6) and TSP-1, have been shown to increase with fibrosis progression in rodent models and patients with liver fibrosis [26, 27]. This suggests that integrins and TSP-1 are likely responsible for TGF-β activation in the advanced stages of liver fibrosis. However, TGF-β activation mediated by these molecules is not detected by an R[58] or L[59] antibody because they activate TGF-β by mechanisms that are different from PLK [8]. As shown in the "Fibrosis" panels of Figs. 6B, C, and 7C, the expression of R[58] and L[59]/LAP-DPs was the highest in patients with fibrosis stage 1 and was decreased in those with stages 2 and 3, suggesting that PLK-dependent TGF-β activation occurs only in the early stages, although total TGF-β activation is increased with the progression of liver fibrosis. Taken together, these findings suggest that PLK may mediate TGF-β activation in the early stages of liver fibrosis, whereas in the advanced stages, different factors, including integrins and TSP-1, may contribute to TGF-β activation, which unfortunately cannot be assessed by an R[58] or L[59] antibody.

Intriguingly, in addition to the ECM, non-parenchymal cells, including HSCs, and some hepatocytes were robustly stained with R[58] antibody (Figs. 3, 4A, and B, fibrosis stage 1B). Recently, glycoprotein A repetitions predominant (GARP), a surface marker of activated regulatory T cells, has been shown to bind latent TGF-β for its activation, which is critical for the cells to suppress effector T cells [28, 29]. In addition, studies have demonstrated that GARP is also present on liver sinusoidal endothelial cells and HSCs [30, 31]. Thus, the R[58]/LAP-DP expression on the cells in our study may reflect the binding of the latent TGF-β complex to the cell surface through GARP and the subsequent PLK-dependent TGF-β activation there.

Our quantitative analysis of the R[58]/LAP-DP expression revealed that NAFLD patients had a significantly higher expression of R[58]/LAP-DP in their liver tissue than patients with chronic viral hepatitis, although the levels of serum markers of liver fibrosis were higher in the latter group (Table 1 and Fig. 6D). This finding may be due to differences in the involvements of PLK and TGF-β in the progression of the two liver diseases. Recently, the endotoxin-induced stimulation of Kupffer cells has been proposed as an important initiating event leading to the onset and progression of NASH [32]. Stimulated Kupffer cells produce tumor necrosis factor-α, which enhances the PLK activity on the HSC surface [33], thereby highlighting the PLK-dependent activation of latent TGF-β in the liver of NAFLD/NASH patients. Conversely, TGF-β signaling events have been reported to show a lower correlation with the fibrosis stage in patients with HCV infection than in those with NAFLD [25]. Instead, the cytokine interleukin-13, which is known to be involved in the fibrosis of diverse organs, was shown to induce HSC activation directly, and its expression was significantly correlated with the severity of liver fibrosis in HCV-infected patients [25]. These reports suggest that the impact of TGF-β signaling may differ depending on the cause of liver diseases and that it may be smaller in cases of HCV-associated liver fibrosis than in NASH-related fibrosis.

The plasma concentration of L[59]/LAP-DP was significantly correlated with the serum ALB level and the FIB-4 value (Figs. 8G and 9C), both of which are indirect markers of liver fibrosis [5, 18, 19, 20], suggesting the association of the plasma L[59]/LAP-DP abundance with the development of liver fibrosis. In contrast, the plasma level of L[59]/LAP-DP showed no correlation with the concentrations of direct serum biomarkers of liver fibrosis, such as HA and Col IV (Fig. 9A and B), presumably due to the different roles of these two types of markers in the progression of liver fibrosis. The L[59]/LAP-DPs are a surrogate marker for PLK-dependent TGF-β activation that induces liver fibrogenesis, and the plasma level increased in the early stages of liver fibrosis but decreased in the advanced stages, while the serum abundance of HA and Col IV is positively correlated with the degree of ECM accumulation and increases with the progression of liver fibrosis [34, 35]. Thus, L[59]/LAP-DPs will serve as a

novel blood marker to evaluate the fibrogenic activity in the liver, independently of widely used serum fibrosis markers.

Studies demonstrated that the TGF-β level after IFN-based treatment was significantly decreased in comparison to before treatment in CHC patients [36, 37, 38, 39]. However, it is controversial whether the abundance of TGF-β or its changes during treatment are associated with virological responses [36, 37, 38, 39, 40, 41]. In most of the studies, the amounts of total TGF-β, including latent LAP-TGF-β complexes, were measured, but the TGF-β activation in the liver was not evaluated precisely [36, 37, 38, 39, 40, 41]. We focused on the PLK-dependent TGF-β activation in this study and examined its association with viral responses to IFN-based therapy by measuring the plasma L[59]/LAP-DP level. The mean concentration of L[59]/LAP-DP in 19 patients with CHC showed a tendency to decrease after the initiation of treatment with PEG-IFN-α and RBV (Fig. 10A). Furthermore, the changes in the plasma L[59]/LAP-DP level during treatment were significantly associated with virological responses (Fig. 10B), although the plasma level itself before and during treatment (after 6 months of treatment) did not predict the treatment outcome (Fig. 10A). These results are consistent with previous reports investigating the relationship between the TGF-β level and the viral response to IFN-based treatment for CHC [36, 40, 41]. TGF-β exerts a proviral effect on HCV replication dependently or independently of its inhibitory actions on IFN signaling [42, 43]. Thus, the bioactive TGF-β level may be positively correlated with the ability of HCV to propagate. Little is known about the mechanisms responsible for the inhibitory effects of IFN-α (plus RBV) on TGF-β activation, except that it inhibits the proliferation of HSCs [44]. Since HCV is reported to increase the TGF-β expression through the induction of reactive oxygen species [45], anti-HCV treatment may also contribute to the suppression of TGF-β activation. In patients with no decreases in their plasma L[59]/LAP-DP level during IFN-based therapy, the inhibitory effects of IFN-α on TGF-β activation and viral propagation could be attenuated due to the possible involvement of host or virus factors in IFN signaling, thus presumably leading to an increase in the number of NRs.

The potential utility of R[58] and L[59]/LAP-DPs as histological and biochemical surrogate markers for the PLK-mediated TGF-β activation will allow for appropriate and prompt interventions for early-stage liver fibrosis. Furthermore, since L[59]/LAP-DP could be a highly sensitive and independent blood marker of liver fibrogenesis, its measurement in combination with other serum fibrosis markers may contribute to the accurate diagnosis and appropriate management of CLD. The recent advent of direct-acting antivirals (DAAs) has led to a major advance in the treatment of hepatitis C, and antiviral therapy with DAAs is now widely used for hepatitis C patients in the world. Thus, we are now studying whether the dynamics of PLK-dependent TGF-β activation observed in patients under IFN-based treatment is also reproduced in those who receive DAA therapy.

Declarations

Author contribution statement

Hiroshi Yokoyama: Conceived and designed the experiments; Performed the experiments; Analyzed and interpreted the data; Wrote the paper.

Takahiro Masaki: Conceived and designed the experiments; Analyzed and interpreted the data; Contributed analysis tools and data; Wrote the paper.

Ikuyo Inoue, Mariko Nakamura: Performed the experiments.

Yoshihiro Mezaki, Kenichi Ikejima: Analyzed and interpreted the data.

Chisato Saeki, Tsunekazu Oikawa, Masayuki Saruta, Hiroyuki Takahashi, Masahiro Ikegami: Contributed materials, analysis tools or data.

Hiroshi Hano: Analyzed and interpreted the data; Contributed reagents, materials, analysis tools and data.

Soichi Kojima: Conceived and designed the experiments; Analyzed and interpreted the data; Contributed reagents, materials, analysis tools and data.

Tomokazu Matsuura: Conceived and designed the experiments; Analyzed and interpreted the data; Contributed reagents, materials and data; Wrote the paper.

Funding statement

Competing interest statement

The authors declare no conflict of interest.

Additional information

No additional information is available for this paper.

Acknowledgements

References

[1] R. Bataller, D.A. Brenner, Liver fibrosis, J. Clin. Invest. 115 (2005) 209−218.

[2] S.L. Friedman, Mechanisms of hepatic fibrogenesis, Gastroenterology 134 (2008) 1655−1669.

[3] S.L. Friedman, Mechanisms of disease: mechanisms of hepatic fibrosis and therapeutic implications, Nat. Clin. Pract. Gastroenterol. Hepatol. 1 (2004) 98−105.

[4] Y. Inagaki, I. Okazaki, Emerging insights into transforming growth factor beta Smad signal in hepatic fibrogenesis, Gut 56 (2007) 284−292.

[5] J.L. Chin, M. Pavlides, A. Moolla, J.D. Ryan, Non-invasive markers of liver fibrosis: adjuncts or alternatives to liver biopsy? Front. Pharmacol. 7 (2016) 159.

[6] N.H. Afdhal, D. Nunes, Evaluation of liver fibrosis: a concise review, Am. J. Gastroenterol. 99 (2004) 1160−1174.

[7] S. Dooley, P. ten Dijke, TGF-beta in progression of liver disease, Cell Tissue Res. 347 (2012) 245−256.

[8] H. Hayashi, T. Sakai, Biological significance of local TGF-beta activation in liver diseases, Front. Physiol. 3 (2012) 12.

[9] R.J. Coffey Jr., L.J. Kost, R.M. Lyons, H.L. Moses, N.F. LaRusso, Hepatic processing of transforming growth factor beta in the rat. Uptake, metabolism, and biliary excretion, J. Clin. Invest. 80 (1987) 750−757.

[10] M. Hara, A. Kirita, W. Kondo, T. Matsuura, K. Nagatsuma, N. Dohmae, et al., LAP degradation product reflects plasma kallikrein-dependent TGF-beta activation in patients with hepatic fibrosis, Springerplus 3 (2014) 221.

[11] M. Hara, I. Inoue, Y. Yamazaki, A. Kirita, T. Matsuura, S.L. Friedman, et al., L(59) TGF-beta LAP degradation products serve as a promising blood biomarker for liver fibrogenesis in mice, Fibrogenesis Tissue Repair 8 (2015) 17.

[12] D.E. Kleiner, E.M. Brunt, M. Van Natta, C. Behling, M.J. Contos, O.W. Cummings, et al., Design and validation of a histological scoring system for nonalcoholic fatty liver disease, Hepatology 41 (2005) 1313−1321.

[13] P. Bedossa, T. Poynard, An algorithm for the grading of activity in chronic hepatitis C. The METAVIR Cooperative Study Group, Hepatology 24 (1996) 289−293.

[14] Z.D. Goodman, Grading and staging systems for inflammation and fibrosis in chronic liver diseases, J. Hepatol. 47 (2007) 598−607.

[15] S. Lepreux, P. Bioulac-Sage, G. Gabbiani, V. Sapin, C. Housset, J. Rosenbaum, et al., Cellular retinol-binding protein-1 expression in normal and fibrotic/cirrhotic human liver: different patterns of expression in hepatic stellate cells and (myo)fibroblast subpopulations, J. Hepatol. 40 (2004) 774−780.

[16] E. Van Rossen, S. Vander Borght, L.A. van Grunsven, H. Reynaert, V. Bruggeman, R. Blomhoff, et al., Vinculin and cellular retinol-binding protein-1 are markers for quiescent and activated hepatic stellate cells in formalin-fixed paraffin embedded human liver, Histochem. Cell Biol. 131 (2009) 313−325.

[17] L. Yang, Y.S. Roh, J. Song, B. Zhang, C. Liu, R. Loomba, et al., Transforming growth factor beta signaling in hepatocytes participates in steatohepatitis through regulation of cell death and lipid metabolism in mice, Hepatology 59 (2014) 483−495.

[18] R.K. Sterling, E. Lissen, N. Clumeck, R. Sola, M.C. Correa, J. Montaner, et al., Development of a simple noninvasive index to predict significant fibrosis in patients with HIV/HCV coinfection, Hepatology 43 (2006) 1317−1325.

[19] S. Sato, T. Genda, T. Ichida, N. Amano, S. Sato, A. Murata, et al., Prediction of hepatocellular carcinoma development after hepatitis C virus eradication using serum *Wisteria floribunda* agglutinin-positive Mac-2-binding protein, Int. J. Mol. Sci. 17 (2016).

[20] A. Vallet-Pichard, V. Mallet, B. Nalpas, V. Verkarre, A. Nalpas, V. Dhalluin-Venier, et al., FIB-4: an inexpensive and accurate marker of fibrosis in HCV infection. Comparison with liver biopsy and fibrotest, Hepatology 46 (2007) 32−36.

[21] E. Miyaki, M. Imamura, N. Hiraga, E. Murakami, T. Kawaoka, M. Tsuge, et al., Daclatasvir and asunaprevir treatment improves liver function parameters and reduces liver fibrosis markers in chronic hepatitis C patients, Hepatol. Res. 46 (2016) 758−764.

[22] M. Yamada, Y. Fukuda, Y. Koyama, I. Nakano, F. Urano, Y. Katano, et al., Serum hyaluronic acid reflects the effect of interferon treatment on hepatic fibrosis in patients with chronic hepatitis C, J. Gastroenterol. Hepatol. 11 (1996) 646−651.

[23] H. Kojima, Y. Hongo, H. Harada, T. Inoue, K. Miyaji, M. Kashiwagi, et al., Long-term histological prognosis and serum fibrosis markers in chronic

hepatitis C patients treated with interferon, J. Gastroenterol. Hepatol. 16 (2001) 1015−1021.

[24] T.M. Chen, P.T. Huang, M.H. Tsai, L.F. Lin, C.C. Liu, K.S. Ho, et al., Predictors of alpha-fetoprotein elevation in patients with chronic hepatitis C, but not hepatocellular carcinoma, and its normalization after pegylated interferon alfa 2a-ribavirin combination therapy, J. Gastroenterol. Hepatol. 22 (2007) 669−675.

[25] H.L. Weng, Y. Liu, J.L. Chen, T. Huang, L.J. Xu, P. Godoy, et al., The etiology of liver damage imparts cytokines transforming growth factor beta1 or interleukin-13 as driving forces in fibrogenesis, Hepatology 50 (2009) 230−243.

[26] Y. Popov, E. Patsenker, F. Stickel, J. Zaks, K.R. Bhaskar, G. Niedobitek, et al., Integrin alphavbeta6 is a marker of the progression of biliary and portal liver fibrosis and a novel target for antifibrotic therapies, J. Hepatol. 48 (2008) 453−464.

[27] G.O. Elpek, G.A. Gokhan, S. Bozova, Thrombospondin-1 expression correlates with angiogenesis in experimental cirrhosis, World J. Gastroenterol. 14 (2008) 2213−2217.

[28] D.Q. Tran, J. Andersson, R. Wang, H. Ramsey, D. Unutmaz, E.M. Shevach, GARP (LRRC32) is essential for the surface expression of latent TGF-beta on platelets and activated FOXP3+ regulatory T cells, Proc. Natl. Acad. Sci. U. S. A. 106 (2009) 13445−13450.

[29] L. Sun, H. Jin, H. Li, GARP: a surface molecule of regulatory T cells that is involved in the regulatory function and TGF-beta releasing, Oncotarget 7 (2016) 42826−42836.

[30] A. Carambia, B. Freund, D. Schwinge, M. Heine, A. Laschtowitz, S. Huber, et al., TGF-beta-dependent induction of CD4(+)CD25(+)Foxp3(+) Tregs by liver sinusoidal endothelial cells, J. Hepatol. 61 (2014) 594−599.

[31] Y. Li, B.G. Kim, S. Qian, J.J. Letterio, J.J. Fung, L. Lu, et al., Hepatic stellate cells inhibit T cells through active TGF-beta1 from a cell surface-bound latent TGF-beta1/GARP complex, J. Immunol. 195 (2015) 2648−2656.

[32] A.J. Wigg, I.C. Roberts-Thomson, R.B. Dymock, P.J. McCarthy, R.H. Grose, A.G. Cummins, The role of small intestinal bacterial overgrowth, intestinal permeability, endotoxaemia, and tumour necrosis factor alpha in the pathogenesis of non-alcoholic steatohepatitis, Gut 48 (2001) 206−211.

[33] K. Akita, M. Okuno, M. Enya, S. Imai, H. Moriwaki, N. Kawada, et al., Impaired liver regeneration in mice by lipopolysaccharide via TNF-alpha/kallikrein-mediated activation of latent TGF-beta, Gastroenterology 123 (2002) 352−364.

[34] S. Takamatsu, H. Nakabayashi, Y. Okamoto, H. Nakano, Noninvasive determination of liver collagen content in chronic hepatitis. Multivariate regression modeling with blood chemical parameters as variables, J. Gastroenterol. 32 (1997) 355−360.

[35] J. Guechot, A. Laudat, A. Loria, L. Serfaty, R. Poupon, J. Giboudeau, Diagnostic accuracy of hyaluronan and type III procollagen amino-terminal peptide serum assays as markers of liver fibrosis in chronic viral hepatitis C evaluated by ROC curve analysis, Clin. Chem. 42 (1996) 558−563. PubMed PMID: 8605673.

[36] I. Kotsiri, E. Hadziyannis, A. Georgiou, M.V. Papageorgiou, I. Vlachogiannakos, G. Papatheodoridis, Changes in serum transforming growth factor-beta1 levels in chronic hepatitis C patients under antiviral therapy, Ann. Gastroenterol. 29 (2016) 79−84. PubMed PMID: 26752952; PubMed Central PMCID: PMC4700851.

[37] E. Janczewska-Kazek, B. Marek, D. Kajdaniuk, H. Borgiel-Marek, Effect of interferon alpha and ribavirin treatment on serum levels of transforming growth factor-beta1, vascular endothelial growth factor, and basic fibroblast growth factor in patients with chronic hepatitis C, World J. Gastroenterol. 12 (2006) 961−965.

[38] R. Flisiak, J. Jaroszewicz, T.W. Lapinski, I. Flisiak, D. Prokopowiczi, Effect of pegylated interferon alpha 2b plus ribavirin treatment on plasma transforming growth factor-beta1, metalloproteinase-1, and tissue metalloproteinase inhibitor-1 in patients with chronic hepatitis C, World J. Gastroenterol. 11 (2005) 6833−6838.

[39] H. Tsushima, S. Kawata, S. Tamura, N. Ito, Y. Shirai, S. Kiso, et al., Reduced plasma transforming growth factor-beta1 levels in patients with chronic hepatitis C after interferon-alpha therapy: association with regression of hepatic fibrosis, J. Hepatol. 30 (1999) 1−7.

[40] D. Roulot, H. Durand, T. Coste, J. Rautureau, A.D. Strosberg, R. Benarous, et al., Quantitative analysis of transforming growth factor beta 1 messenger RNA in the liver of patients with chronic hepatitis C: absence of correlation between high levels and severity of disease, Hepatology 21 (1995) 298−304.

[41] B. Marek, D. Kajdaniuk, U. Mazurek, E. Janczewska-Kazek, B. Kos-Kudla, B. Strzalka, et al., TGF-beta1 mRNA expression in liver biopsy specimens and TGF-beta1 serum levels in patients with chronic hepatitis C before and after antiviral therapy, J. Clin. Pharm. Ther. 30 (2005) 271−277.

[42] W. Lin, E.M. Weinberg, A.W. Tai, L.F. Peng, M.A. Brockman, K.A. Kim, et al., HIV increases HCV replication in a TGF-beta1-dependent manner, Gastroenterology 134 (2008) 803−811.

[43] T. Shirasaki, M. Honda, T. Shimakami, K. Murai, T. Shiomoto, H. Okada, et al., Impaired interferon signaling in chronic hepatitis C patients with advanced fibrosis via the transforming growth factor beta signaling pathway, Hepatology 60 (2014) 1519−1530.

[44] A. Mallat, A.M. Preaux, S. Blazejewski, J. Rosenbaum, D. Dhumeaux, P. Mavier, Interferon alfa and gamma inhibit proliferation and collagen synthesis of human Ito cells in culture, Hepatology 21 (1995) 1003−1010.

[45] W. Lin, W.L. Tsai, R.X. Shao, G. Wu, L.F. Peng, L.L. Barlow, et al., Hepatitis C virus regulates transforming growth factor beta1 production through the generation of reactive oxygen species in a nuclear factor kappaB-dependent manner, Gastroenterology 138 (2010) 2509−2518, 18 e1.